Synthesis and Evolution of PbS Nanocrystals through a Surfactant-Assisted Solvothermal Route

Chao Zhang, Zhenhui Kang, Enhong Shen, Enbo Wang,* Lei Gao, Fang Luo, Chungui Tian, Chunlei Wang, and Yang Lan

Institute of Polyoxometalate Chemistry, Department of Chemistry, Northeast Normal University, Changchun 130024, P. R. China

Jixue Li and Xuejing Cao

State Key Laboratory of Inorganic Synthesis and Preparative Chemistry, Jilin University, Changchun 130012, P. R. China

Received: June 14, 2005; In Final Form: October 28, 2005

We present a surfactant-assisted solvothermal approach for the controllable synthesis of a PbS nanocrystal at low temperature (85 °C). Nanotubes (400 nm in length with an outer diameter of 30 nm), bundle-like long nanorods (about 5−15 μm long and an average diameter of 100 nm), nanowires (5−20 μm in length and with a diameter of 20−50 nm), short nanorods (100−300 nm in length and an axial ratio of 5−10), nanoparticles (25 nm in width with an aspect ratio of 2), and nanocubes (a short axis length of 10 nm and a long axis length of 15 nm) were successfully prepared and characterized by transmission electron microscopy, scanning electron microscopy, and powder X-ray diffraction pattern. A series of experimental results indicated that several experimental factors, such as AOT concentration, ratio of [water]/[surfactant], reaction time, and ratio of the reagents, play key roles in the final morphologies of PbS. Possible formation mechanisms of PbS nanorods and nanotubes were proposed.

Introduction

Lead sulfide (PbS) is an important $\pi-\pi$ semiconductor material with a small band gap (0.41 eV, in bulk form at 300 K) and a large exciton Bohr radius (18 nm). It has been widely used in many fields such as in Pb^{2+} ion-selective sensors,[1] photography,[2] IR detectors,[3] solar absorbers,[4] and optical switch.[5] In the limit of strong confinement, the third-order nonlinear optical response of PbS nanocrystals is expected to be 30 times larger than that of GaAs and 1000 times larger than that of CdSe materials, thus rendering PbS nanocrystals highly desirable for photonic and optical switching device applications.[6,7] Moreover, it has long been found that the size and morphology of compound II−VI semiconductors strongly affect their properties and applications.[8−11] Consequently, obtaining PbS nanocrystals with different morphologies is potentially meaningful in finding novel applications of such kinds of semiconductors.

PbS nanocrystals have been prepared in polymers,[12] in mesoporous silica SBA-15,[13] in block copolymer nanoreactors,[14] and on ultrathin polydiacetylene templates,[15] through electrodeposited,[16] solvothermal route,[17,18] microbial method,[19] hydrothermal process,[20] and electroporation of vesicles.[21] PbS has several different morphologies, such as quantum dots, nanoparticles, nanorods,[22,23] hierarchical nanostructures,[24,25] star-shape nanocrystals,[26] composite nanotubes of PbS nanoparticles,[27] and so on. Until now, the synthesis of multi-morphology PbS nanocrystals with controllable shape and size is still a very important and interesting topic. Here, we focus on the controlled synthesis and evolution of PbS nanocrystals, which are carried out by an AOT-assisted solvothermal route.

* To whom correspondence should be addressed. Tel: +86-431-5098787. Fax: +86-431-5098787. E-mail: wangenbo@public.cc.jl.cn.

Surfactant-assisted synthesis of nano- and microstructured inorganic materials has attracted considerable interest because of its effective soft template effect, reproducibility, and simple maneuverability.[28−30] In this paper, a simple AOT-assisted solvothermal method is used for the controllable synthesis of various PbS nanocrystals. Through control of several experimental parameters (such as the concentration of the surfactant, ratio of [water]/[surfactant], ratio of the reagents, and the reaction time), the final morphology of the products is effectively controlled and interesting results are achieved. In our experiments, nanotubes, -cubes, -particles, and -rods are successfully produced with a high yield and low size distributions. To our best knowledge, pure PbS nanotubes are reported here for the first time.

Experimental Section

In this work, all reagents were of analytical grade and used without further purification. $Pb(AOT)_2$ was prepared through ion exchange with the sodium salt as described elsewhere.[12] In a typical experiment, a small quantity of thiourea (TAA) solution (0.10 mol/L) was added into a 10 mL isooctane solution containing 0.001 mol of AOT (sodium dioctyl sulfosuccinate), and then 0.05 mol/L $Pb(AOT)_2$ solution in isooctane was injected. Afterward, all of the above solution was transferred into a 15 mL Teflon-lined stainless steel autoclave, sealed, and maintained at 85 °C for 12 h. The collected products were then washed with absolute ethanol several times and dried under vacuum at 60 °C.

The transmission electron microscopy (TEM) images and electron diffraction (ED) patterns were obtained on a JEM-2010 (200 kV) and JEM-3010 (300 kV). Scanning electron microscopy (SEM) images were obtained on a scanning electron

10.1021/jp053215+ CCC: $33.50
Published on Web 12/08/2005

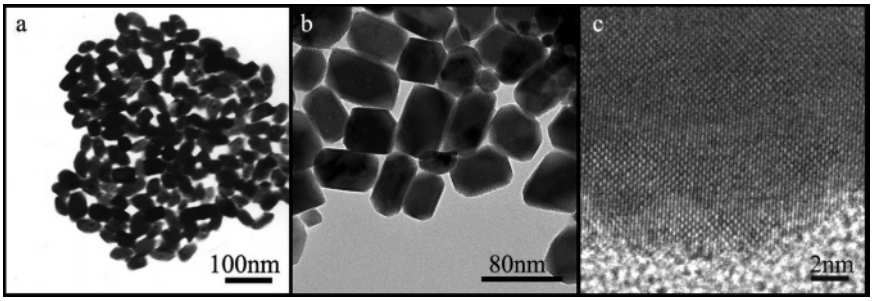

Figure 1. (a) Low magnification TEM image of the nanoparticles prepared at AOT concentration = 0.10 mol/L, $w = 10$, reaction time = 12 h, (b) higher magnification TEM image, and (c) HRTEM image of a single nanoparticle.

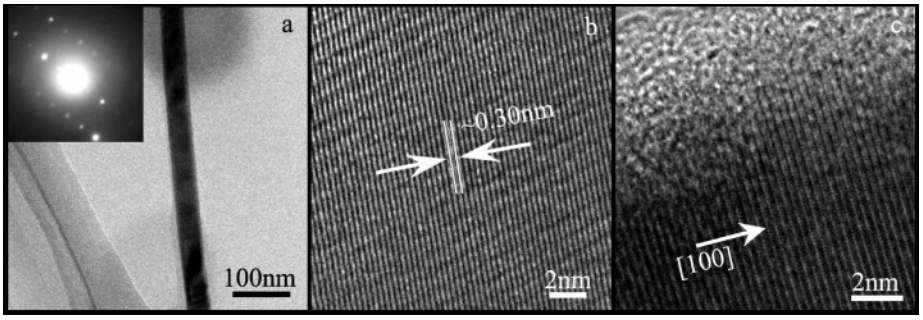

Figure 2. (a) TEM image of a single nanowire prepared at AOT concentration = 0.10 mol/L, $w = 10$, reaction time = 24 h, (b and c) HRTEM images of the nanowire.

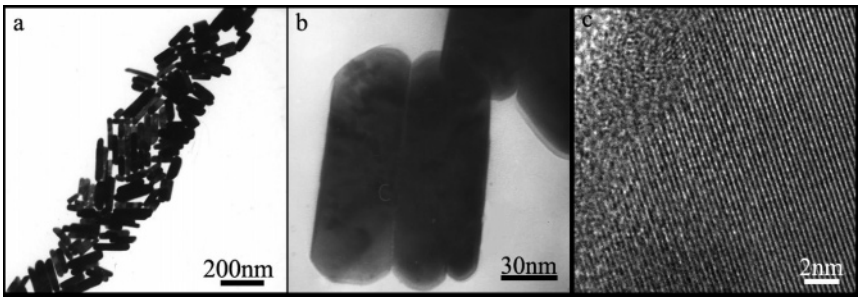

Figure 3. (a) Low magnification TEM image of nanorods prepared at AOT concentration = 0.12 mol/L, $w = 10$, reaction time = 12 h, (b) higher magnification TEM image of the nanorods, and (c) HRTEM image of a nanorod.

microscope, Hitachi, ×650/EDAX, PV9100. X-ray power diffraction (XRD) patterns of the products were recorded on a Rigaku D/max γ_A X-ray diffractometer equipped with graphite monochromatized Cu Kα radiation ($\lambda = 0.154178$ nm) at a scan rate of 0.02 °/s in the range of 20−70°.

Results and Discussion

1. Effect of "*w*", AOT Concentration, Reagent Ratio, and Reaction Time. In this work, various PbS nanostructures can be obtained easily by changing the experimental parameters. Their main morphologies are nanoparticles, nanorods, nanowires, nanotubes, and nanocubes. The details of relations of the final morphologies and the experimental parameters are shown in Table S1 (see Supporting Information). Figure 1a shows the typical TEM images of as-prepared nanoparticles with a high yield (90%) and a low size distribution (reaction time 12 h). It can be seen that the particles are about 50 nm in length and probably 25 nm in width. The higher magnification TEM image is shown in Figure 1b. The HRTEM image of the nanoparticles in Figure 1c and the good lattice fringes illustrate these nanoparticles are single crystalline. When the reaction time was prolonged under the same condition, PbS nanowires can be obtained as well as the nanoparticles, and the nanowires quantity increased as the reaction time went on. Figure 2a displays a single nanowire with a diameter of probably 50 nm (ED pattern inset image). The nature of the single crystalline of the nanowires is revealed by HRTEM as seen in parts b and c of Figure 2. The fringe spacing is estimated to be 0.30 nm, which is close to the [200] lattice spacing of PbS, indicating that the crystal growth is preferential in the [100] direction. This growth pattern has also been observed by Qian's group[18] and Yang and Wang.[12] The short nanorods synthesized at a higher surfactant concentration (0.12 mol/L) are shown in Figure 3. Figure 3 gives the TEM images at different magnifications and HRTEM image, respectively. As it can be seen, the length is about 100−200 nm and the width is 20−50 nm. The clear lattice fringes in the HRTEM image confirm the high crystallinity of the nanorods. When sequentially changing the dosage of AOT, cubic nanoparticles and novel nanotubes appear which are, respectively, shown in Figure 4. Figure 4a clearly shows that the cubic nanoparticles have a small size distribution. They have a long axis range from 15 to 20 nm and a short axis range from 8 to 15 nm. The ED pattern (inset Figure S4) confirms the nanocubes are single crystalline. Parts b, c, and d of Figure 4 show TEM images of the interesting PbS nanotubes at different magnifications, respectively. These nanotubes are approximately 400 nm in length, with an outside diameter of 30 nm and an inside diameter of 25 nm with sealed ends (more TEM images of PbS

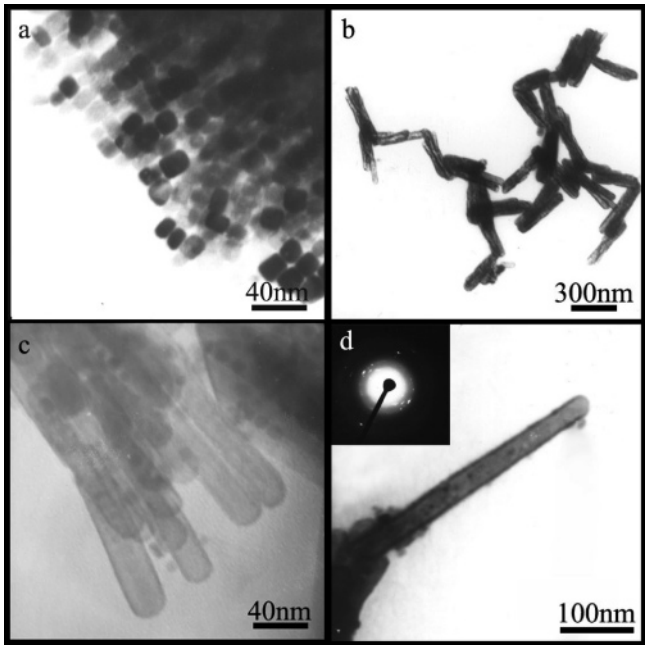

Figure 4. TEM images of the nanocubes and nanotubes prepared at AOT concentration = 0.18 mol/L, $w = 10$, reaction time = 24 h, (a) TEM image of the nanocubes, (b and c) TEM images of the naotubes, and (d) TEM image of a single nanotube and the ED pattern.

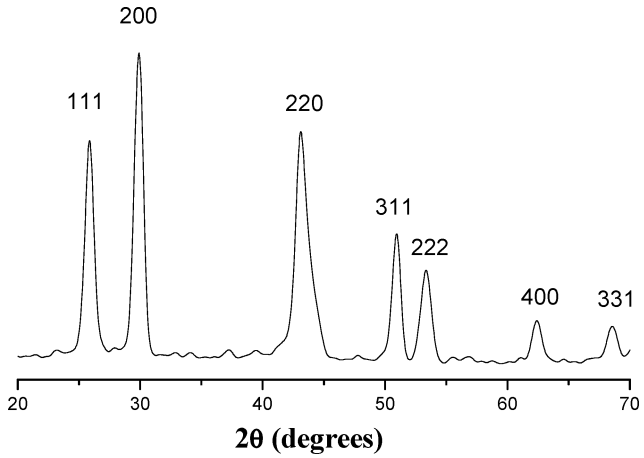

Figure 5. XRD pattern of PbS nanoparticles prepared at 0.10 mol/L AOT, $w = 10$, reaction time = 12 h.

nanotubes are shown in the Supporting Information.). From the electron diffraction pattern shown in Figure 4d (inset), we find that the nanotubes are single crystalline.

The XRD pattern of the nanoparticles (shown in Figure 5) shows sharp peaks corresponding to cubic PbS with an fcc rock-salt structure (JCPDS 5-592), indicating that the nanoparticles are well crystallized. The major seven peaks can be indexed as 111, 200, 220, 311, 222, 400, and 331, respectively. No peaks of other impurities were detected.

Series experiments are carried out to find a suitable *w* value in this synthetic system. The *w* value is changed from 5 to 20 with other parameters fixed. The typical results are as follows. When $w = 5$, the products are nanoparticles with a wide size distribution (from 20 to 200 nm). When $w = 8$, the products are short rods with 80−100 nm in width and 100−200 nm in length as shown in Figure 3a. When *w* ranges from 10 to 15, all the products are rodlike nanoparticles similar to those shown in Figure 1a. When $w = 20$, the products with multi-morphologies and various sizes can be obtained, such as nanoparticles, spheres, nanocubes, nanorods, and so on. In our

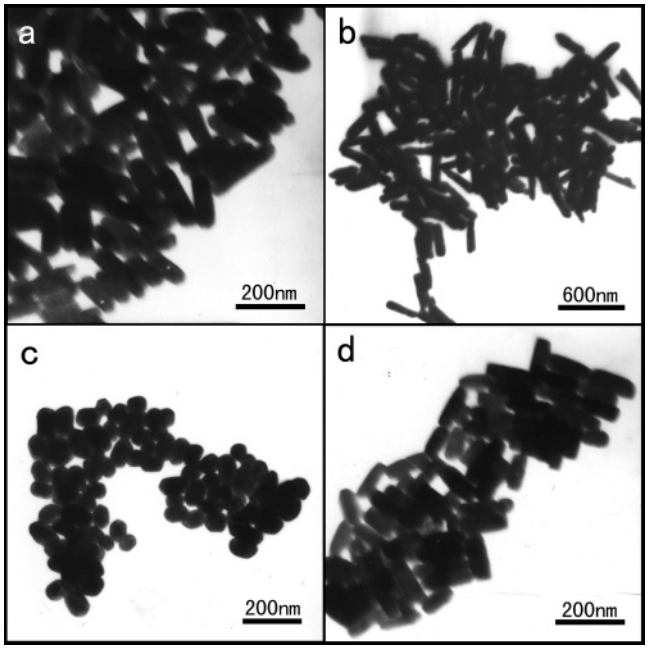

Figure 6. TEM images of the products prepared employing various AOT concentrations: (a) 0.14 mol/L and (b) 0.16 mol/L and reagent ratio, (c) 0.6 mL of $Pb(AOT)_2$ solution and (d) 0.2 mL of $Pb(AOT)_2$ solution.

experiments, it is found that the optimized condition was $w = 10$, which leads to the high yield and low size distribution. The following series of experiments that were carried out at "w" = 10 exhibit that the sizes and morphologies of the final products are strongly dependent on the ratios of the reagents. While the concentration of TAA is increased from 0.10 to 0.15 mol/L, with the same reaction time (for example reaction time = 12 h), nanorods similar to those shown Figure 3a could be obtained. The typical morphologies of the products which are obtained by using a $Pb(AOT)_2$ solution of 0.6 and 0.2 mL are shown in parts c and d of Figure 6, respectively. Under the same conditions, a higher ratio of [TAA]/[$Pb(AOT)_2$] leads to the increased size and aspect ratio.

Much research focuses on reverse micelles and microemulsion, which indicates that the surfactant has important efficacy in controlling the size, shape, and crystallinity of inorganic nanocrystals.[31] In this work, the concentration of the AOT strongly affects the morphologies of the products. Nanoparticle, nanorods, nanotubes, and nanocubes are obtained through simply adjusting the concentration of AOT from 0.10 to 0.18 mol/L. Figure 1a presents the nanoparticles as prepared when AOT = 0.10 mol/L. The rodlike particles are about 25 nm in width with an aspect ratio of 2. When the AOT concentration is increased to 0.12 mol/L, the products are short rods as shown in Figure 3a. By increasing the AOT concentration to 0.14 mol/L, the obtained products (shown in Figure 6a) become longer and a little bigger than the previous ones. When AOT concentration is up to 0.16 mol/L, as can be seen in Figure 6b, the nanorods acquired their length of 300 nm and an aspect ratio of 5. When a higher concentration of AOT (0.18 mol/L) is used, nanotubes and nanocubes can be obtained. On the basis of the above results, it can be seen that the length and aspect ratio of the PbS nanocrystals increase when enhancing the AOT concentration from 0.10 to 0.18 mol/L. The possible reasons are as follows. First, a frequently encountered behavior of longer-chain surfactants is that, at low intermediate concentrations, the viscosity will rapidly increase with the increase in concentration. Under different concentrations, AOT molecules may assemble

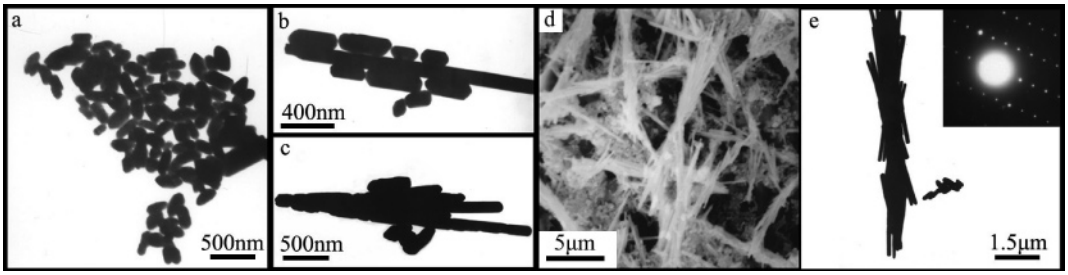

Figure 7. TEM and SEM images of PbS prepared at various times: (a) 12 h, (b) 30 h, (c) 36 h, and (d and e) 48 h.

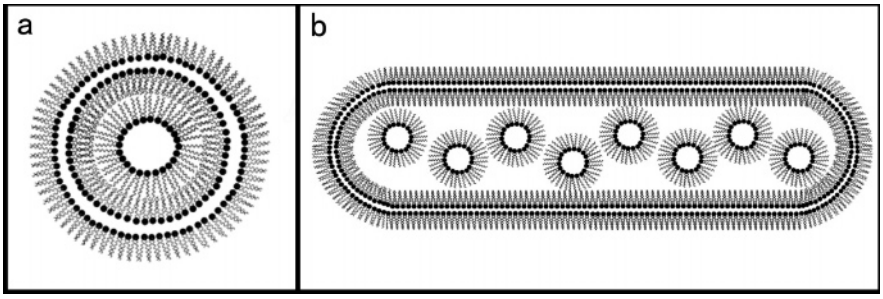

Figure 8. Schematic illustration of a possible micelle: (a) the cross section of the short axis, (b) the cross section along the long axis.

to different aggregates with various size and shape. In the present system, with the increase of concentration, the AOT aggregates transfer from short prolate to cylinders shapes.[32,33] Second, the system is a dynamic one, in that the surfactants involved in the formation of the micelles can leave the aggregates and are replaced by the reagent molecules that freely move in the aqueous bulk phase.[31] Furthermore, the surfactants can absorb on the surface of nanoparticles through crystal-face-specific interactions. The interactions among themselves will influence the nanocrystals growth rate and growth direction.[34]

Reaction time is another important factor that can affect the morphology of the products. Samples obtained at a different reaction time at 85 °C are shown in Figure 7. In Figure 7a, TEM images show that the samples (the reaction time 12 h) as obtained are nanoparticles. When the reaction time is prolonged, the long rods appear and their quantity increases with increasing reaction time. The SEM image in Figure 7d and TEM image in Figure 7e show the morphology of the as synthesized products with a reaction time of 48 h. Here, most of the products are long rods. This can be explained by the fact that longer growth times could lead to the formation of a nanocrystal that is thermodynamically stable.[35]

2. Possible Mechanism. The process of reactions can be expressed as the following reaction equations

$$NH_2CSNH_2 + 2H_2O \rightarrow NH_4^+ + H_2S + CH_3COO^-$$

$$Pb^{2+} + S^{2-} \rightarrow PbS$$

2.1. Formation of Nanopaticle and Nanorod. AOT is a twin-tailed surfactant and is most commonly used to make microemulsions. In the AOT/isooctane/water system, the hydrocarbon chains tend to self-associated to minimize contact with the water molecules, resulting in the formation of various aggregates,[36] which then lead to the formation of reverse micelles with a different shape. The system is dynamic, in that the surfactants involved in the formation of micelles leave the aggregates and are replaced by others that freely move in the aqueous bulk phase. These are helpful to the formation of products with similar shapes. What should be mentioned is that the concentration of AOT is within the range from 0.10 to 0.16 mol/L, the size and shape of the products are not strictly determined by the form of the micelles which should be prolate or rodlike. Presumably, a nucleation process of the droplets containing Pb^{2+} and S^{2-} takes place. However, as previously reported, AOT selectively adsorbs on a certain facet of the crystal and this leads to a preferential growth of this facet, resulting in the formation of elongated nanoparticles. The elongated nanoparticles are dynamically coated by AOT and aggregate by the interaction of the organic molecules. It has been reported that such a process could readily occur, for example, in the presence of surface-anchored surfactant molecules.[27,34,38] These thus formed nanoparticles then act as building blocks to produce further assemblies which finally lead to the formation of products with other kinds of shapes. If the two adjacent nanoparticles linked and could be maintained, a longer one "nanoparticle" could then yield. Meanwhile, other Pb^{2+} and S^{2-} could join in the growth process along this direction and finally lead to the formation of long rods.[39−48] Such a presumption can be verified by the phenomenon that, as the reaction time passes, the percentage of long rods in the total products increases and the diameter of the long rods is kept approximately equal to the width of the original nanoparticles, as shown in parts b and c of Figure 7. The TEM images shown in Figure 7 are obtained from the products isolated at different growth times, after the reaction was going on for 12, 30, 36, and 48 h, respectively. The ED pattern inset in Figure 7e reveals the single-crystalline nature of the long nanorods. The morphologies for the PbS nanocrystals evolution are shown in TEM and SEM images, which provide powerful evidence for the above speculation.

2.2. Formation of Nanotube and Nanocube. As proposed above, the shapes of the AOT aggregate in the system could transform with the change of the concentration of AOT. Within a relatively low concentration (0.10−0.16 mol/L in this system), the aggregates should be rodlike or have a cylinder shape. When confined within a sealed system at 85 °C, AOT molecules in a higher AOT concentration (0.18 mol/L for example) solution could aggregate to form an interesting model similar to the onion-like lamellar phase,[31] as depicted in Figure 8.[31,49−50] A conjectural process is that the presence of plentiful surfactant molecules and NH_4^+ in the above-mentioned sealed system[51−54]

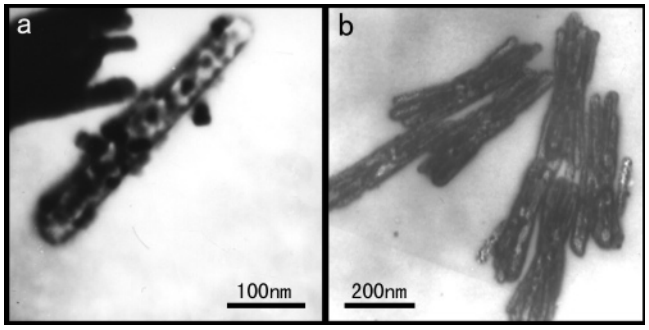

Figure 9. TEM images of the products employing at different times: (a) 18 h and (b) 22 h.

made the micelles acquire different interesting structures compared to those under common conditions. With a rodlike morphology, the water pool within the micelles may be divided into two parts. One part is in the region that is similar to the shell of a peanut. Another part is in the sphere micelles. As shown in Figure 8, the relationship between them is just like a peanut shell to a peanut.

In the experimental process, it is found that PbS nanocubes and nanotubes coexisted in the same reaction system. As a presumption, they may be synthesized based on the soft templates, as depicted above, and the growth of them should experience the following courses. First, nucleation takes place in the water pool confined by the aggregates of the surfactants. The small volume of the interior water pool made the effect of selective absorbtion on specific crystal facets small and thus resulted in the formation of cubic nanoparticles mirroring the fundamental cubic crystal structure of the galena unit cell in the surfactant aggregates as depicted in Figure 8.[55] Second, when the nanocubes that exist in the internal nanotubes grow to an enough size (just as shown in Figure 4a), they break away from the micelles and self-assemble through the interactions between the capping AOT molecules. After a period of aging time, the surface of the nanotubes then turned smooth. TEM images of nanocubes and nanotubes isolated from different phases are shown in Figure 9. When the reaction time is 18 h, products shown in Figure 9a can be obtained. It can be seen that some nanocubes exist in the interior of the originally formed nanotubes. Figure 9b is the morphology of the products taken 22 h after the reaction started.

Conclusions

In summary, a series of PbS nanostructures are synthesized using a facile solvothermal method at a low temperature and on a large scale. Through precise control of the experimental parameters, PbS nanocrystals with different morphologies are all obtained with a high yield. The obtained nanotubes and very small nanocubes may bring promising applications for PbS nanocrystals. On the basis of the experimental results, valid mechanisms of the growth of PbS nanocrystals in the employed experimental systems were given and this may provide a useful guide for future synthesis of other nanostructures in AOT systems.

Acknowledgment. Financial support was provided by the National Natural Science Foundation of China (20371011).

Supporting Information Available: TEM images of PbS nanotubes, nanocubes, nanotube bundles, and nanowires. HR-TEM images of a nanowire. Table demonstrating the relationships between experimental parameters and the products. This material is available free of charge via the Internet at http://pubs.acs.org.

References and Notes

(1) Hirata, H.; Higashiyama, K. *Bull. Chem. Soc. Jpn.* **1971**, *44*, 2420.
(2) Nair, P. K.; Gomezdaza, O.; Nair, M. T. S. *Adv. Mater. Opt. Electron.* **1992**, *1*, 139.
(3) Gadenne, P.; Yagil, Y.; Deutscher, G. *J. Appl. Phys.* **1989**, *66*, 3019.
(4) Chaudhuri, T. K.; Chatterjes, S. *Proc. Int. Conf. Thermoelectr.* **1992**, *11*, 40.
(5) Kane, R. S.; Cohen, R. E.; Silbey, R. *J. Phys. Chem.* **1996**, *100*, 7928.
(6) Hines, M. A.; Scholes, G. D. *Adv. Mater.* **2003**, *15*, 1844.
(7) Sargent, E. H. *Adv. Mater.* **2005**, *17*, 515.
(8) Colvin, V. L.; Schlamp, M. C.; Alivisatos, A. P. *Nature* **1994**, *370*, 354.
(9) Klein, D. L.; Roth, R.; Lim, A. K. L.; Alivisatos, A. P.; McEuen, P. L. *Nature* **1997**, *389*, 699.
(10) Ridley, B. A.; Nivi, B.; Jacobson, J. M. *Science* **1999**, *286*, 746.
(11) Ahmadi, T. S.; Wang, Z. L.; Green, T. C.; Henglein, A.; EI-Sayed, M. A. *Science* **1996**, *272*, 1924.
(12) Wang, S.; Yang, S. *Langmuir* **2000**, *16*, 389.
(13) Gao, F.; Lu, Q. Y.; Liu, X. Y.; Yan, Y. S.; Zhao, D. Y. *Nano Lett.* **2001**, *1*, 743.
(14) Kane, R. S.; Cohen, R. E.; Silbey, R. *Chem. Mater.* **1996**, *8*, 1919.
(15) Berman, A.; Belman, N.; Golan, Y. *Langmuir* **2003**, *19*, 10962.
(16) Nanda, K. K.; Sahu, S. N. *Adv. Mater.* **2001**, *13*, 280.
(17) Tang, K. B.; Qian, Y. T.; Zeng, J. H.; Yang, X. G. *Adv. Mater.* **2003**, *15*, 448.
(18) Yu, D. B.; Wang, D. B.; Meng, Z. Y.; Lu, J.; Qian, Y. T. *J. Mater. Chem.* **2002**, *12*, 403.
(19) Kowshik, M.; Vogel, W.; Uran, J.; Kulkarni, S. K.; Paknikar, K. M. *Adv. Mater.* **2002**, *14*, 815.
(20) Kuang, D. B.; Xu, A. W.; Fang, Y. P.; Liu, H. Q.; Frommen, C.; Fenske, D. *Adv. Mater.* **2002**, *15*, 1747.
(21) Wu, S. X.; Zeng, H. X.; Schelly, Z. A. *Langmuir* **2005**, *21*, 687.
(22) Mo, M. S.; Shao, M. W.; Hu, H. M.; Yang, L.; Yu, W. C.; Qian, Y. T. *J. Cryst. Growth* **2002**, *244*, 364.
(23) Wan, J. X.; Chen, X. Y.; Wang, Z. H.; Yu, W. C.; Qian, Y. T. *Mater. Chem. Phys.* **2004**, *88*, 217.
(24) Ma, Y. R.; Qi, L. M.; Ma, J. M.; Cheng, H. M. *Cryst. Growth Des.* **2004**, *4*, 351.
(25) Ni, Y. H.; Liu, H. J.; Wang, F.; Liang, Y. Y.; Hong, J. M.; Ma, X.; Xu, Z. *Cryst. Growth Des.* **2004**, *4*, 759.
(26) Lee, S. M.; Jun, Y. W.; Cho, S. N.; Cheon, J. W. *J. Am. Chem. Soc.* **2002**, *124*, 11244.
(27) Leontidis, E.; Orphanou, M.; Kyprianidou-Leodidou, T.; Krumeich, F.; Caseri, W. *Nano Lett.* **2003**, *3*, 569.
(28) Kang, Z. H.; Wang, E. B.; Jiang, M.; Lian, S. Y. *Nanotechnology* **2004**, *15*, 55.
(29) Kang, Z. H.; Wang, E. B.; Jiang, M.; Lian, S. Y.; Li, Y. G.; Hu, C. W. *Eur. J. Inorg. Chem.* **2003**, 370.
(30) Cao, M. H.; Hu, C. W.; Wang, E. B. *J. Am. Chem. Soc.* **2003**, *125*, 11196.
(31) Pileni, M. P. *Nat. Mater.* **2003**, *2*, 145.
(32) Nolmberg, K.; Jönsson, B.; Kronberg, B.; Lindman, B. *Surfactants And Polymers In Aqueous Solution*, 2nd ed.; Wiley: Hoboken, NJ, 2003; Chapter 3.
(33) Pileni, M. P. *Langmuir* **1997**, *13*, 3267.
(34) Cölfen, H.; Mann, S. *Angew. Chem., Int. Ed.* **2003**, *42*, 2350.
(35) Lee, S. M.; Cho, S. N.; Cheon, J. W. *Adv. Mater.* **2003**, *15*, 441.
(36) Evans, D. F.; Mitchell, D. J.; Ninham, B. W. *J. Phys. Chem.* **1986**, *90*, 2817.
(37) Wang, Z. L. *Adv. Mater.* **1998**, *10*, 13.
(38) Peng, X. G.; Manna, L.; Yang, W.; Wickham, J.; Scher, E.; Kadavanich, A.; Alivisatos, A. P. *Nature* **2000**, *404*, 59.
(39) Tang, Z. Y.; Kotov, N. A.; Giersig, M. *Science* **2002**, *297*, 237.
(40) Peng, Z. A.; Peng, X. G. *J. Am. Chem. Soc.* **2002**, *124*, 3343.
(41) Li, M.; Schnablegger, H.; Mann, S. *Nature* **1999**, *402*, 393.
(42) Li, F.; Ding, Y.; Gao, P. X.; Xin, X. Q.; Wang, Z. L. *Angew. Chem.* **2004**, *116*, 5350.
(43) Sun, Y. G.; Mayers, B.; Herricks, T.; Xia, Y. N. *Nano Lett.* **2003**, *3*, 955.
(44) Wiley, B.; Sun, Y. G.; Mayers, B.; Xia, Y. N. *Chem.−Eur. J.* **2005**, *11*, 454.
(45) Xia, Y. N.; Yang, P. D.; Sun, Y. G.; Wu, Y. Y.; Mayers, B.; Gates, B.; Yin, Y. D.; Kim, F.; Yan, H. Q. *Adv. Mater.* **2003**, *15*, 353.
(46) Zhang, D. F.; Sun, L. D.; Yin, J. L.; Yan, C. H. *Adv. Mater.* **2003**, *15*, 1022.
(47) Peng, X. G. *Adv. Mater.* **2003**, *15*, 459.
(48) Peng, Q.; Dong, Y. J.; Li, Y. D. *Angew. Chem., Int. Ed.* **2003**, *42*, 3027.

(49) Ma, Y. R.; Qi, L. M.; Ma, J. M.; Cheng, H. M. *Adv. Mater*. **2004**, *16*, 1023.
(50) Xiong, Y. J.; Xie, Y.; Yang, J.; Zhang, R.; Wu, C. Z.; Du, G. A. *J. Mater. Chem.* **2002**, *12*, 3712.
(51) Rao, C. N. R.; Govindaraj, A.; Leonard Deepak, F.; Gunari, N. A.; Nath, M. *Appl. Phys. Lett.* **2001**, *78*, 1853.
(52) Faeder, J.; Albert, M. V.; Ladanyi, B. M. *Langmuir* **2003**, *19*, 2514.
(53) Fioretto, D.; Freda, M.; Onori, G.; Santucci, A. *J. Phys. Chem. B* **1999**, *103*, 8217.
(54) Riter, R. E.; Undiks, E. P.; Levinger, N. E. *J. Am. Chem. Soc.* **1998**, *120*, 6062.
(55) Gou, L. F.; Murphy, C. J. *Nano Lett.* **2003**, *2*, 231.